

Optimal pre-conditioning and support designs of floor heave in deep roadways

Chunlai Wang^{*1,2}, Guangyong Li^{1,2a}, Ansen Gao^{1,2b}, Feng Shi^{1,2c}, Zhijiang Lu^{1,2d} and Hui Lu^{1,2e}

¹Faculty of Resources & Safety Engineering, China University of Mining & Technology Beijing 100083, China

²Coal Industry Engineering Research Center of Top-coal Caving Mining, Beijing, 100083, China

(Received October 13, 2016, Revised May 3, 2017, Accepted September 3, 2017)

Abstract. In order to reduce deformation of roadway floor heave in deep underground soft rockmass, four support design patterns were analyzed using the Fast Lagrangian Analysis of Continua (FLAC)3D, including the traditional bolting (Design 1), the bolting with the backbreak in floor (Design 2), the full anchorage bolting with the backbreak in floor (Design 3) and the full anchorage bolting with the bolt-grouting backbreak in floor (Design 4). Results show that the design pattern 4, the full anchorage bolting with the bolt-grouting backbreak in floor, was the best one to reduce the deformation and failure of the roadway, the floor deformation was reduced at 88.38% than the design 1, and these parameters, maximum vertical stress, maximum horizontal displacement and maximum horizontal stress, were greater than 1.69%, 5.96% and 9.97%. However, it was perfectly acceptable with the floor heave results. The optimized design pattern 4 provided a meaningful and reliable support for the roadway in deep underground coal mine.

Keywords: numerical simulation; soft rock roadway; rock bolt supporting; roadway stability

1. Introduction

In deep mining, there are many large strains in rockmass induced by high original stresses. Under the high stress conditions, the deformation phenomena are easily generated, such as the roof subsidence, the sidewall convexity and the floor heave. These problems are so serious for personnel safety and mining production in deep coal mining, the effective roadway support design is raising concerns in recent years (Chang and Xie 2011, Lu *et al.* 2011, Shen 2014, Li *et al.* 2015, Kang *et al.* 2014, Gao *et al.* 2016, Saleem 2015, Lee 2016, Yang and Yan 2015). To solve these support problems, the proposed design pattern, especially the roadway floor deformation, was considered one of the most important problems in the mining process. In the last decade, due to the time-lag effect and the complexity of the actual deformation measurement, numerical methods have been widely applied in geotechnical engineering (Shen 2014, Xia *et al.* 2014, Kang *et al.* 2014, Basirat *et al.* 2015, Xing *et al.* 2008, Saksala

2014, Lu *et al.* 2015, Chen *et al.* 2015, Vlachopoulos and Diederichs 2014). It suggests that this could be used to solve many scientific problems in roadway support. Many researchers established different types of numerical models for studying the roadway support, and many results were obtained, such as a trigon logic model and a new friction angle and failure mode using Universal Distinct Element Code (UDEC) (Gao and Stead 2014), a numerical model about the failure mechanism and stability control mechanism of deep coal roadway by UDEC (Chen *et al.* 2016), the optimal support pattern (Yu *et al.* 2013), and a numerical algorithm for simulating jointed rock masses' discontinuous deformation (Chen *et al.* 2016). Actually, there is a good correlation between the results derived from numerical simulations and the realistic mechanic properties of rock material (Hamdi *et al.* 2014, Zhang *et al.* 2013). Using numerical method, the soft coal roadways along the floor were more stable comparing the floor and roof respectively (Liu *et al.* 2010). Numerical model was used to obtain the rockmass stress reconstructs characteristics after protective coal seam exploitation (Zhang *et al.* 2014), the performance stability of haulage roadway were evaluated using numerical method (Abdellah 2015), a direct measurement of pre-mining stress field was obtained using numerical method (McKinnon 2001), and a excavation method was used to design roadway supporting (Jia and Wang 2008). Based on the deformation, an effective method was developed to reduce the soft rock deformation using ANSYS (Tian *et al.* 2013), and the rock bolt-grouting strengthening method was put forward for the surrounding soft rockmass roadway using FLAC3D (Kang *et al.* 2012). Using the comparative analysis of numerical simulation, the reasonable parameters of the high strength support were obtained and applied (Feng *et al.* 2013). Based on this, numerical simulation is provided an effective method to

*Corresponding author, Associate Professor
E-mail: tswcl@126.com

^aGraduate Student
E-mail: liguangyong@student.cumtb.edu.cn

^bGraduate Student
E-mail: gaoansen@student.cumtb.edu.cn

^cGraduate Student
E-mail: shifeng@student.cumtb.edu.cn

^dGraduate Student
E-mail: luzhijiang@student.cumtb.edu.cn

^eGraduate Student
E-mail: luhui@student.cumtb.edu.cn

solve the roadway floor deformation.

In this paper, using the FLAC3D, a numerical model of roadway supporting was established. The stress field, the displacement field and the supporting effect were compared in four support design patterns. The design patterns were used to evaluate the roadway floor heave in Da'anshan coal mine, Beijing, China. The obtained results could provide a meaningful and interesting reference for the roadway floor heave in deep coal mining.

2. Geological and geotechnical conditions

In Da'anshan coal mine, the longwall method is adopted to mining at 900 m depth. The lithological descriptions of rock units in Da'anshan coal mine is shown in Fig. 1. The first coal seam, marked as #13, has a thickness varying from 0.77 m to 2.53 m. Below the #13 coal seam, the material is comprised of a sandy conglomerate with a thickness varying between 0.1 m and 0.2 m. Below the sandy conglomerate lies the #12 coal seam, with a thickness varying from 0.64 m to 2.41 m. Below the #12 coal seam lies a layer of siltstone and sandstone with a thickness of 0.65 m to 1.14 m. The #10 coal seam is below the siltstone and sandstone, with a thickness ranging from 0 m to 7.41 m. Below the #10 coal seam, there is a layer of siltstone and sandstone with a thickness of 1.35 m to 2.78 m. Below this layer of siltstone and sandstone lies the #9 coal seam with a thickness of 0 m to 4.4 m. The #9 coal seam was currently being mined using the longwall mining method. The coal measure stratum, within total thickness of 494.5-820 m and average thickness of 559.5 m, is composed of 56.4% arenaceous shale, 26.18% fine-sandstone, 5.81% coal and 11.61% metamorphic rock. The overburden terrane contains many complex geological structures, such as folds and faults. Both the coal seam and surrounding rock strata are extremely cracked and weak due to the high ground stress. In this coal mine, the floor heave is difficult to be solved, and is serious to threaten the mining personnel safety and mining production.

Thickness (m)	Column	Lithology	Geological descriptions
0.77-2.53 1.5	█	Coal # 13	Medium hard, semibright, unstable
0.1-0.2	██	Sandy conglomerate	Ash black, fine-grained filling
0.64-2.41 1.3	█	Coal # 12	Medium hard, semibright, unstable
0.65-1.14 0.8	██	Siltstone, sandstone	Ash black, argillaceous cement
0-7.41 1.42	█	Coal # 10	Medium hard, unstable from semidull to semibright
1.35-2.78 1.7	██	Siltstone, sandstone	Ash black, argillaceous cement
0-4.40 1.76	█	Coal # 9	Medium hard, dirt band semibright, unstable
3.15-6.18 4.5	██	Siltstone, sandstone	Ash black, argillaceous cement
0.83-6.08 2.44	█	Coal # 7	Medium hard, semibright, unstable
1.02-3.2 1.7	██	Sandstone	Ash black, argillaceous cement
0-10.63 1.05	█	Coal # 6	Medium hard, extremely unstable, from semidull to semibright
1.5-5.8 4.2	██	Siltstone, sandstone	Ash black, argillaceous cement

Fig. 1 Lithological descriptions of rock units in Da'anshan coal mine

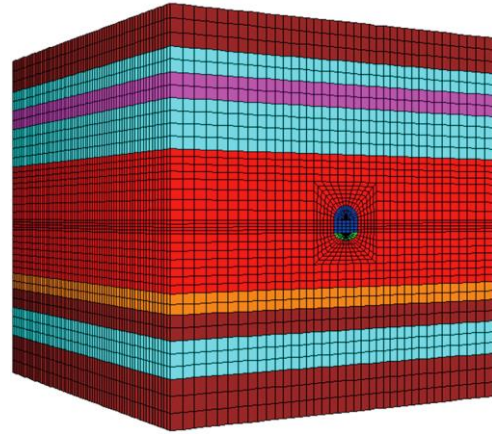
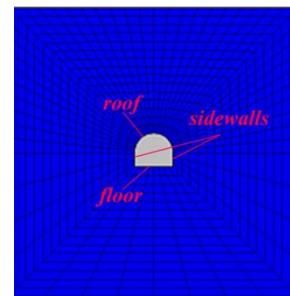
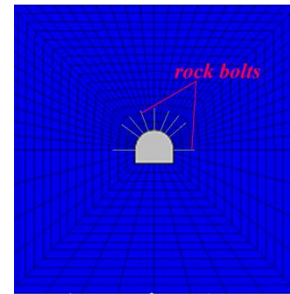


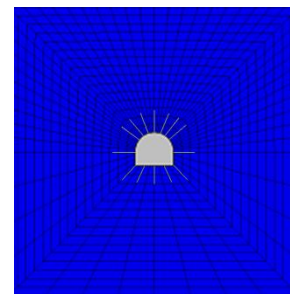
Fig. 2 Numerical calculation model



(a) Sketch of roadway model without supporting



(b) Sketch of roadway model with traditional rock bolt supporting



(c) Sketch of roadway model with full enclosed rock bolt supporting

Fig. 3 Numerical model of roadway

Table 1 Physical and mechanics parameters of rock stratum in the model

Rock stratum	Thickness (m)	Density (kg/m ³)	Elastic modulus (MPa)	Poisson ratio	Cohesion (MPa)	Friction angle(°)	Tensile strength (MPa)
fine-sandstone	5	2690	1000	0.25	1.5	40	0.13
arenaceous shale	3	2660	900	0.22	1.4	41	0.13
two-layer coal	3	1520	500	0.3	1.1	36	0.06

Table 1 Continued

Rock stratum	Thickness (m)	Density (kg/m ³)	Elastic modulus (MPa)	Poisson ratio	Cohesion (MPa)	Friction angle(°)	Tensile strength (MPa)
arenaceous shale	6	2660	900	0.22	1.4	41	0.13
arenaceous shale	17	2660	700	0.2	1.2	40	0.1
four-layer coal	2.5	1520	500	0.3	1.1	36	0.06
fine-sandstone	3	2690	1000	0.25	1.5	40	0.13
arenaceous shale	4.5	2660	900	0.22	1.4	41	0.13
fine-sandstone	6	2690	1000	0.25	1.5	40	0.13

3. Numerical simulations

3.1 Numerical model

The FLAC3D software was used to simulate the roadway excavation. Based on the practical geological conditions of the roadway in the Da'anshan coal mine, the model was built. The critical properties of the rockmass were listed in Table 1. As shown in Fig. 2, the whole model contains 124880 units. The boundary conditions were set as follows. All the units were bound by sliding hinge at the horizontal directions. The bottom boundary of the model was fix hinge, while the upper boundary was free in vertical direction. The roadway was simulated with the shape of horseshoe, with the area size of roadway sidewall and floor is 4 m × 4 m, and the arch radius of roadway roof is 2 m. The model is a size of 56 m in strike length, 50 m in width and 50 m in height. The roadway was at a depth of 900 m. The horizontal stress was set to be 42.3 MPa along the strike direction and 35.8 MPa along the dip direction.

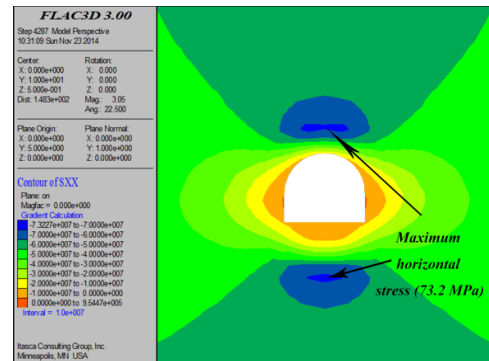
As shown in Fig. 3(a)-3(c), the excavated roadway with or without the rock bolt support was proposed. The roadway was supported without rock bolt as shown in Fig. 3(a). The rock bolt distribution was shown in Fig. 3(b) and 3(c). The rock bolts were installed at roof and sidewalls of the roadway as shown in Fig. 3(b), and the rock bolts were installed at roof, sidewalls and floor as shown in Fig. 3(c). The length of the pre-tensioned rock bolts was 2.4 m, the diameter was 22 mm and the pre-tensioned force was 70 kN, respectively. The interval of anchor rock bolts was 0.8 m.

3.2 Numerical simulation steps

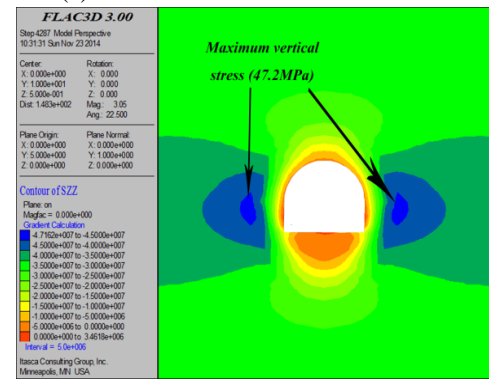
In the numerical model, the excavation along the strike direction of roadway was carried out step by step according to the design. Four roadway supporting patterns were applied, including the traditional bolting (Design 1), the bolting with the backbreak in floor (Design 2), the full anchorage bolting with the backbreak in floor (Design 3) and the full anchorage bolting with the bolt-grouting backbreak in floor (Design 4). The simulated results were obtained under different support patterns, such as the deformation, the stress and the plastic zone of soft rockmass roadway. The following results were based on the excavation of 20 m along the strike direction of roadway.

4. Results and analysis

4.1 The traditional bolting pattern

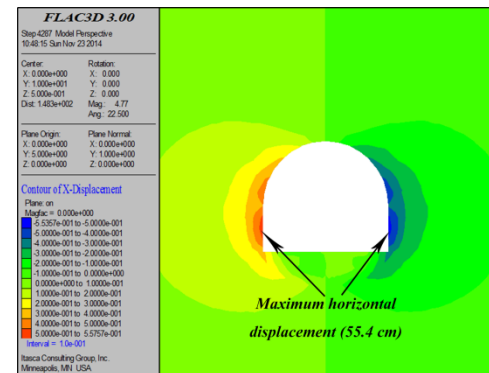


(a) The horizontal stress distribution

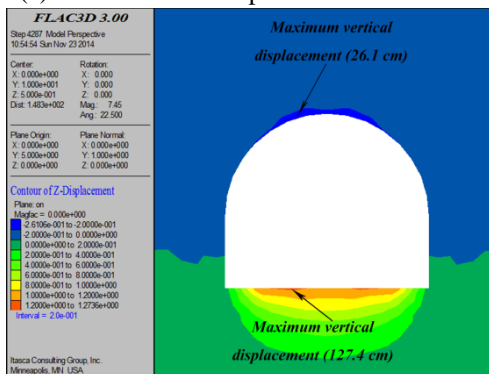


(b) The vertical stress distribution

Fig. 4 The stress distribution of roadway under traditional bolting pattern



(a) The horizontal displacement distribution



(b) The vertical displacement distribution

Fig. 5 The displacement distribution around roadway under traditional bolting pattern

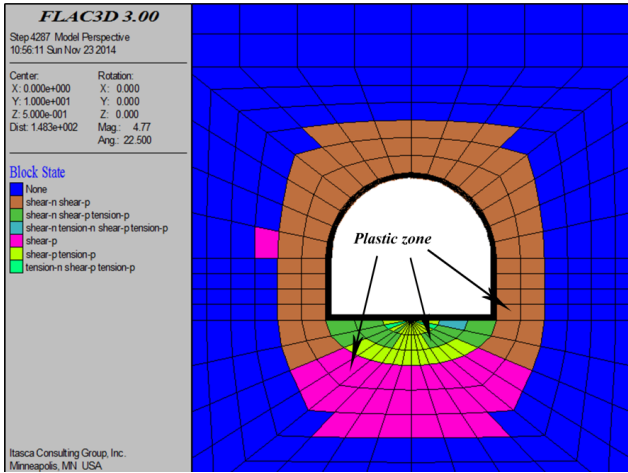
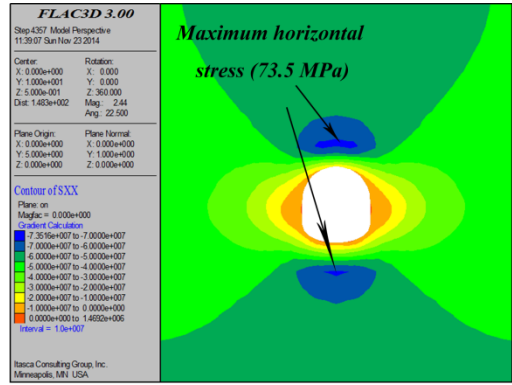
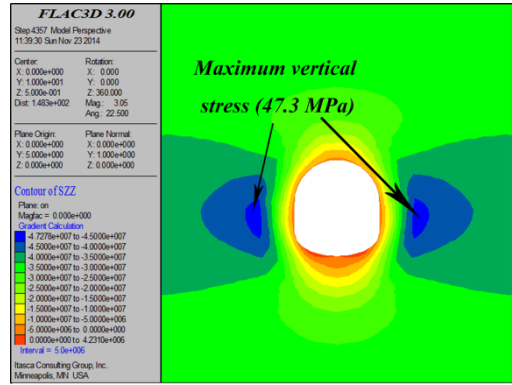


Fig. 6 The plastic zone distribution around roadway under traditional bolting pattern

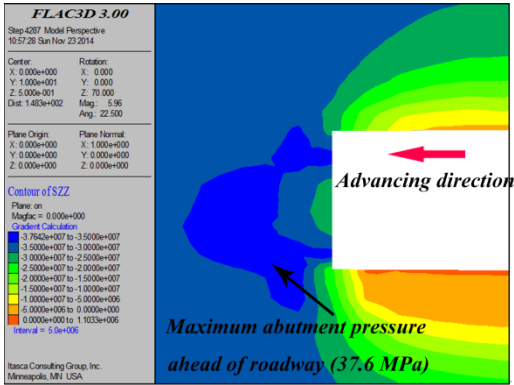


(a) The horizontal stress distribution

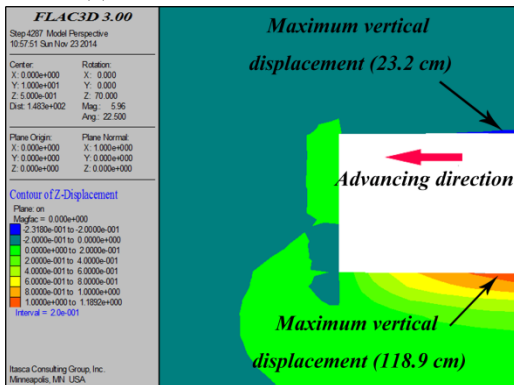


(b) The vertical stress distribution

Fig. 8 The stress distribution around the traditional bolting roadway with backbreak in floor



(a) The vertical stress distribution



(b) The vertical displacement distribution

Fig. 7 The stress and displacement distribution on the section plane of roadway along the strike at 20 m

In this supporting design pattern, rock bolts were installed in the roof and sidewalls of the roadway, and there was no control in the floor, as shown in Fig. 3(b). The horizontal and vertical stress distributions were shown in Fig. 4. The horizontal stress was concentrated on the inner of roof and floor of roadway, and the maximum horizontal stress was 73.2 MPa. By contrast, the vertical stress was concentrated at the roadway sidewalls, and the vertical stress was large enough to be 47.2 MPa. However, the vertical stress at the floor, which indicated that the floor was in pressure relief state, was much lower.

As shown in Fig. 5, because of the roadway strengthened by rock bolts, the maximum horizontal displacement was approximate 55.4 cm in the sidewalls, but the maximum vertical displacement was approximate 127.4 cm in the floor. As shown in Fig. 6, it also revealed that the plastic zone of floor extended wider than that of roadway in this supporting design pattern.

As shown in Fig. 7, the influence scope of the abutment pressure ahead of roadway was revealed from the section plane along the strike direction after workface 20 m. The abutment pressure ahead of roadway was 37.6 MPa. The maximum displacement of the roof was 23.2 cm, and the maximum displacement of the floor was 118.9 cm.

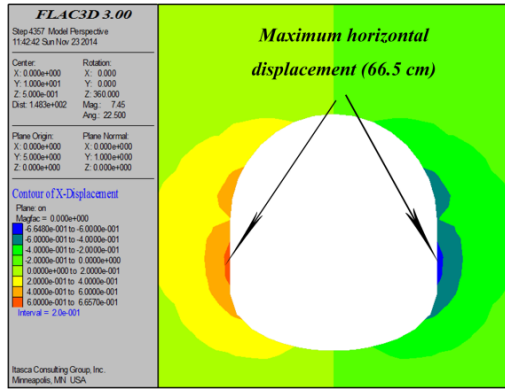
4.2 The traditional bolting with the backbreak in floor

In this supporting design pattern, the roof and the sidewalls of roadway were strengthened by rock bolts. As shown in Fig. 8, the horizontal and vertical stress distributions of the roadway were similar with that in the traditional supporting design listed in the section 4.1. However, an arched pressure area was formed at the roof and roadway sidewalls. As shown in Fig. 9, the maximum horizontal displacement of the roadway sidewalls was 66.5 cm. However, the maximum vertical displacement of the floor was even to 46.4 cm. As shown in Fig. 10, the depth and area of plastic zone at the backbreak in floor of the roadway were smaller than the traditional support pattern. As shown in Fig. 11, the stress and displacement distributions were shown on the section plane along the

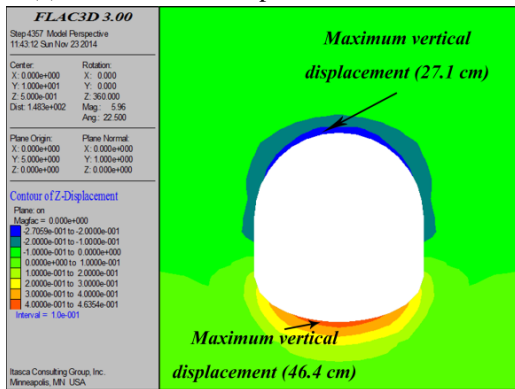
strike direction of roadway at 20 m. The abutment pressure ahead of roadway was 37.4 MPa. The maximum displacement of the roof was 24.2 cm, and the maximum displacement of the floor was 46.4 cm.

4.3 The full anchorage bolting with the backbreak in floor

In this supporting design pattern, the roof, sidewalls and the floor of roadway were strengthened by the full anchorage of rock bolts. To make better contrast with the



(a) The horizontal displacement distribution



(b) The vertical displacement distribution

Fig. 9 The displacement distribution around the traditional bolting roadway with backbreak in floor

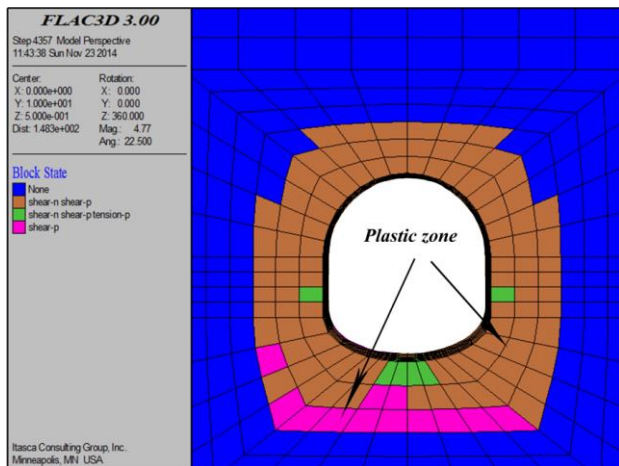
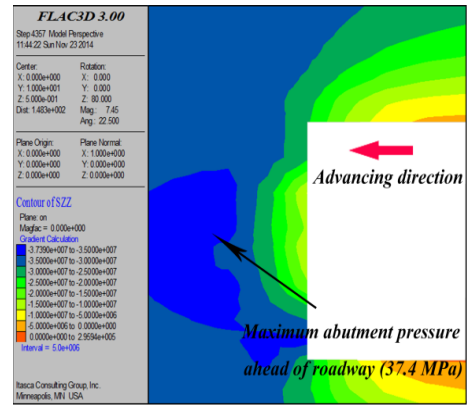
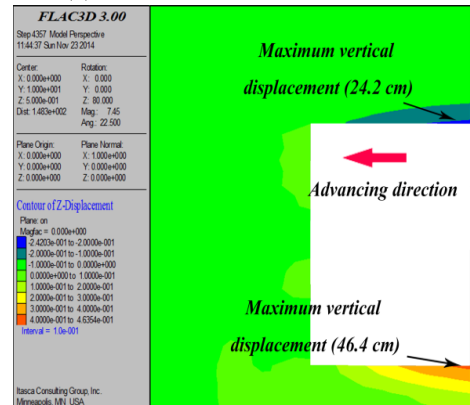


Fig. 10 The plastic zone distribution around the traditional bolting roadway with backbreak in floor

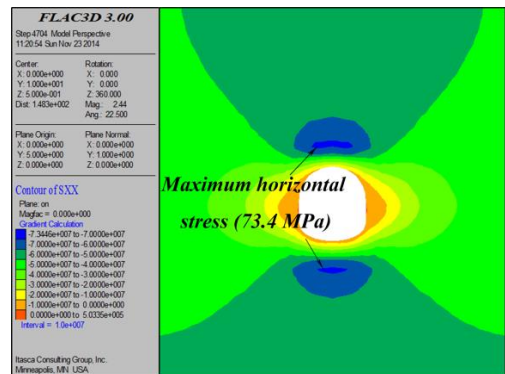


(a) The vertical stress distribution

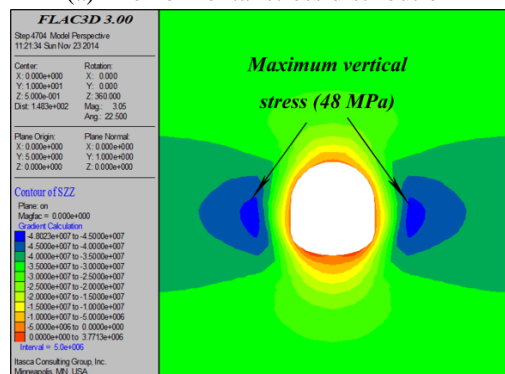


(b) The vertical displacement distribution

Fig. 11 The stress and displacement distribution on the section plane along the strike of roadway at 20 m

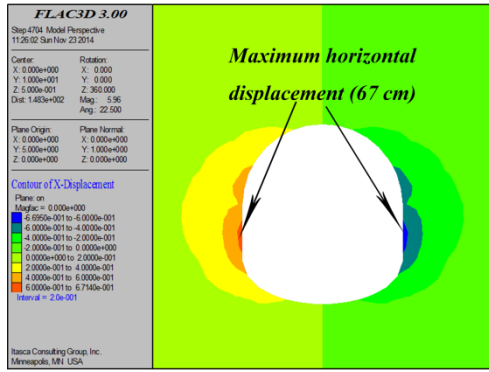


(a) The horizontal stress distribution

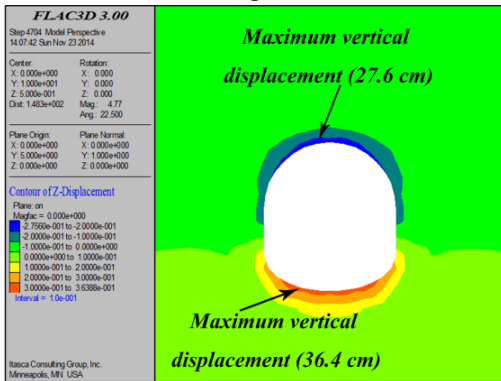


(b) The vertical stress distribution

Fig. 12 The stress distribution around the full anchorage bolting roadway with the backbreak in floor

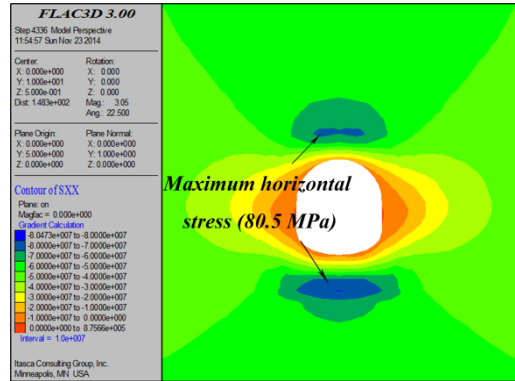


(a) The horizontal displacement distribution

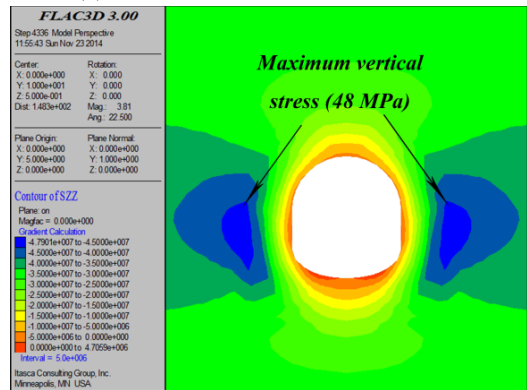


(b) The vertical displacement distribution

Fig. 13 The displacement distribution around the full anchorage bolting roadway with the backbreak in floor



(a) The horizontal stress distribution



(b) The vertical stress distribution

Fig. 15 The stress distribution around the full anchorage bolting roadway with the bolt-grouting backbreak in floor

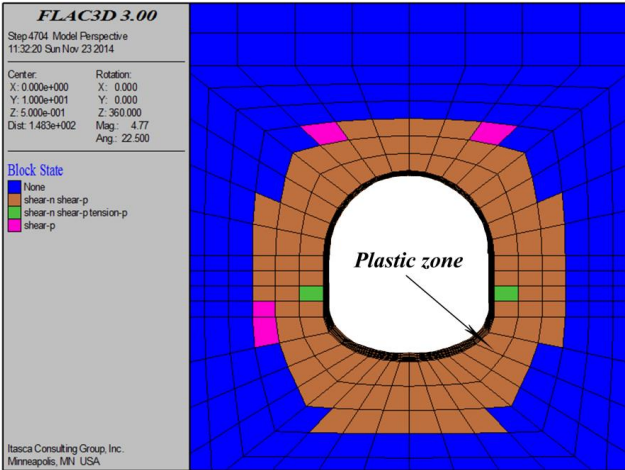
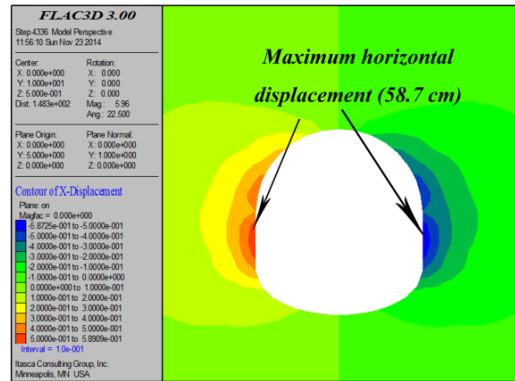
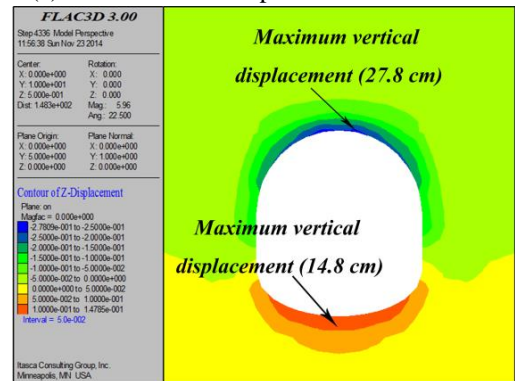


Fig. 14 The plastic zone distribution around the full anchorage bolting roadway with the backbreak in floor



(a) The horizontal displacement distribution



(b) The vertical displacement distribution

Fig. 16 The displacement distribution around the full anchorage bolting roadway with the bolt-grouting backbreak in floor

other designs pattern, the stress status and deformation distribution were analyzed in this study, respectively. The roadway was excavated and supported by the full anchorage bolting with the backbreak in floor. Figs. 12 and 13 showed the stress and displacement distributions in the full anchorage bolting roadway with the backbreak in floor. The maximum vertical displacement of floor reduced to be 36.4 cm, as shown in Fig. 13. The scopes of plastic zone of the roadway were decreased, as shown in Fig. 14.

4.4 The full anchorage bolting with bolt-grouting backbreak in floor

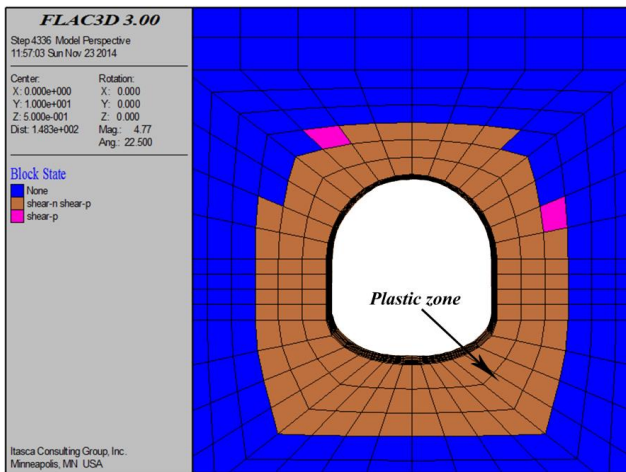


Fig. 17 The plastic zone distribution around the full anchorage bolting roadway with the backbreak in floor

In this supporting design, the roof and the sidewalls of roadway were strengthened by rock bolts, while the backbreak in floor was reinforced by bolt-grouting. In order to acquire the stress and deformation distribution of the full anchorage bolting roadway with the bolt-grouting backbreak in floor, Figs. 15 and 16 showed respectively the stress and the displacement distributions using this support design pattern. As shown in Fig. 15, the stress distribution was similar as that of Fig. 12, and an arched pressure area was formed obviously by vertical stress. In terms of displacement distribution in the Fig. 16, the maximum deformation of floor reduced from 127.4 cm to 14.8 cm comparing with that in the traditional support design. This indicated that the deformation of floor was reduced in this design. Meanwhile, the maximum deformation of the roof was 27.8 cm, which may not vary with the maximum floor displacement mentioned in the section 4.3. As shown in Fig. 16, the maximum deformation of the roadway sidewalls was 58.7 cm using this design. Fig. 17 showed that the area of plastic zone of the roadway decreased greater.

5. Discussions

The comparison results of the four supporting design patterns were shown in Fig. 18. The maximum vertical displacement of the backbreak in floor roadway decreased by 63.6% than that of flat bottom roadway whose maximum value was 127.4 cm. Comparing the data as shown in Figs. 6-10, the area of plastic zone around the backbreak in floor roadway reduced greatly. The results showed that the backbreak in floor was beneficial for the stability of roadway. This might be related with the more released deformation energy through the backbreak in floor. The backbreak in floor was used to strengthen the floor non-deformability and redistribute the stress around the roadway. In the process of the reinforcement, a portion of energy transferred from the floor to the roof and the sidewalls. As shown in Fig. 9, the maximum horizontal displacement of roadway sidewalls was 66.5 cm, and the roof was 27.1 cm. It was little larger than that of the flat bottom roadway mentioned in the design 1, as shown in Fig. 5. The full anchorage bolting could be improved by the

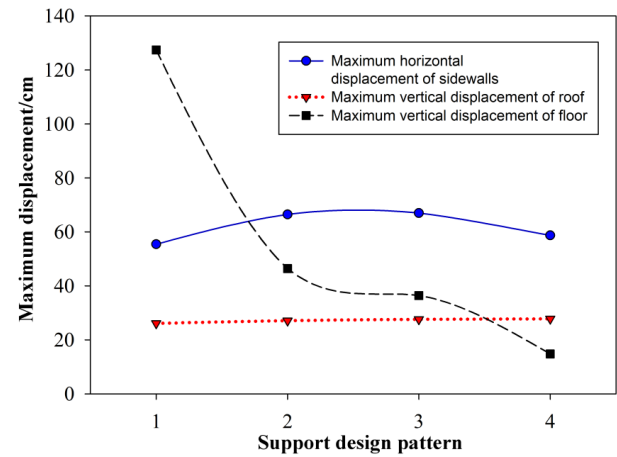


Fig. 18 The comparison results of four supporting design patterns

load-carrying capacities of roadway. The rock bolt application may be provided by some experiences to design the roadway supporting pattern. The integral overlying strata by the bolting, and the composite beams can be formed to support the roadway. The rock bolt support can effectively increase the cohesion and friction angle of rockmass. As shown in Figs. 9-13, the optimized design of the full anchorage bolting for the backbreak in floor was proposed in the sections 4.1 and 4.2. The results showed that the pre-tensioned bolting were better in the field. However, it cannot prevent the deformation of the roadway only by adopting the high-strength support method because the soft rock roadway stored high deformation energy. The plastic zone of in the soft rock roadway still carried a strong bearing capacity. It was worthy to take full advantage of the residual strength of surrounding rockmass.

Thus, it may have a good effect when the bolt-grouting was applied to the surrounding rockmass strength. As shown in Fig. 18, the floor deformation in design 4 was reduced at 88.38% than that in the design 1, and these parameters, maximum vertical stress, maximum horizontal displacement and maximum vertical stress, were greater than 1.69%, 5.96% and 9.97%. The results indicated that the design pattern 4 was effective in reducing the displacement of the roadway. However, it was perfectly acceptable with the floor heave results. The proposed design pattern 4 was an optimal support design for reducing displacement of roadway in deep soft rock mass.

6. Conclusions

In this study, four roadway support designs were simulated and used to analyze the stress and deformation distribution of roadway surrounding rock mass using the FLAC3D software. The main conclusions are listed in the following:

- The backbreak in floor plays an important role in the reducing of floor deformation.
- Obtaining technological benefits, the design 3 and 4, the full anchorage bolting method with the backbreak in floor and the full anchorage bolting method with the bolt-

grouting backbreak in floor, are much better than the others. Especially design 4 is the optimal design to support the requirements of large roadway deformation.

- Upon the large deformation of surrounding rockmass, the floor deformation of roadway should be reduced firstly. Using the method of design 4, the floor deformation could be reduced effectively.

The results showed that the design 4 was very prominent for the floor heave in deep underground roadways. Obtaining more perfectly results, we proposed the design pattern 4. This may improve the quality of disposal floor heave. Finally, we recommend the design pattern 4 on reducing displacement of floor heave for future research.

Acknowledgements

We thank the National Natural Science Foundation of China (No. 51374217, 51574246), the National Key Research and Development Project (No. 2017YFC0804201), the Yue Qi Distinguished Scholar Project, China University of Mining & Technology, Beijing, the Fundamental Research Funds for the Central Universities (No. 2011QZ01).

References

- Abdellah, W. (2015), "Numerical modelling stability analyses of haulage drift in deep underground mines", *J. Eng. Sci. Assiut Univ.*, **43**(1), 71-81.
- Basirat, R., Niri, G.A. and Izadifard, R.A. (2015), "The effect of sand layer thickness and moisture content on underground structures behavior due to surface blasting", *J. Eng. Res.*, **3**(4), 31-42.
- Chang, J.C. and Xie, G.X. (2011), *Investigation on Deformation and Failure Characteristics and Stability Control of Soft Rock Roadway Surrounding Rock in Deep Coal Mine*, in *Advanced Materials Research*, Trans Tech Publications, 3711-3716.
- Chen, W., Konietzky, H. and Abbas, S. (2015), "Numerical simulation of time-independent and -dependent fracturing in sandstone", *Eng. Geol.*, **193**, 118-131.
- Chen, M., Yang, S.Q., Zhang, Y.C. and Zang, C.W. (2016), "Analysis of the failure mechanism and support technology for the Dongtan deep coal roadway", *Geomech. Eng.*, **11**(3), 401-420.
- Chen, Y.J., Zhu, W.S., Li S.C. and Zhang, X. (2016), "New reinforcement algorithms in discontinuous deformation analysis for rock failure", *Geomech. Eng.*, **11**(6), 787-803
- Feng, J.C., Li, H.J., Zhao, Z.C. and Zhang, W.L. (2013), *New Type of High-Strength Support in Deep Soft Rock Roadway*, in *Advanced Materials Research*, Trans Tech Publications, 1520-1525.
- Gao, F.Q. and Stead, D. (2014), "The application of a modified Voronoi logic to brittle fracture modelling at the laboratory and field scale", *J. Rock Mech. Min. Sci.*, **68**, 1-14.
- Gao, S.M., Chen, J.P., Zuo, C.Q., Wang, W. and Yang, S. (2016), "Structure optimization for the support system in soft rock tunnel based on numerical analysis and field monitoring", *Geotech. Geol. Eng.*, **34**(4), 1089-1099.
- Hamdi, P., Stead, D. and Elmo, D. (2014), "Damage characterization during laboratory strength testing: A 3D-finite-discrete element approach", *Comput. Geotech.*, **60**, 33-46.
- Jia, J.P. and Wang, H.T. (2008), "Stability analysis of tunnel support based on site survey and numerical simulation", *Proceedings of the 2008 International Workshop on Modelling, Simulation and Optimization WMSO'08*, Hong Kong, December.
- Kang, H.P., Lin, J. and Fan, M.J. (2015), "Investigation on support pattern of a coal mine roadway within soft rocks-a case study", *J. Coal Geol.*, **140**, 31-40.
- Kang, Y.S., Liu, Q.S., Gong, G.Q. and Wang, H.C. (2014), "Application of a combined support system to the weak floor reinforcement in deep underground coal mine", *J. Rock Mech. Min. Sci.*, **71**, 143-150.
- Kang, Z.Q., Yan, S.H. and Yan, Q. (2012), *The Study of Numerical Simulation about Roadway Bolting and Reinforcement to Jointed Rock Mass*, in *Advanced Materials Research*, 159-162.
- Lee, Y.J. (2016), "Determination of tunnel support pressure under the pile tip using upper and lower bounds with a superimposed approach", *Geomech. Eng.*, **11**(4): 587-605
- Li, S.C., Wang, Q., Wang, H.T., Jiang, B., Wang, D.C., Zhang, B., Li, Y. and Ruan, G.Q. (2015), "Model test study on surrounding rock deformation and failure mechanisms of deep roadways with thick top coal", *Tunn. Undergr. Sp. Technol.*, **47**, 52-63.
- Liu, J.J., Lu, J.T. and Li, Z.H. (2010), "Numerical analysis for anchoring of surrounding rock of thick soft coal roadway", *Proceedings of the 2010 International Conference on Mechanic Automation and Control Engineering (MACE)*, Wuhan, China, June.
- Lu, H.F. (2015), "Stress and displacement analysis of aerial oil & gas pipelines: A case study of Lantsang tunnel crossing project", *J. Eng. Res.*, **3**(3), 141-156.
- Lu, X.L., Liu, Q.S. and Su, P.F. (2010), "Deformation mechanism and support measures for stress-induced cracked rock mass of deep coal mine roadway", *Proceedings of the International Symposium on Geomechanics and Geotechnics: From Micro to Macro*, Shanghai, China, October.
- McKinnon, S.D. (2001), "Analysis of stress measurements using a numerical model methodology", *J. Rock Mech. Min. Sci.*, **38**(5), 699-709.
- Saksala, T. (2014), "Rate-dependent embedded discontinuity approach incorporating heterogeneity for numerical modeling of rock fracture", *Rock Mech. Rock Eng.*, **48**(4), 1605-1622.
- Saleem, M. (2015), "Application of numerical simulation for the analysis and interpretation of pile-anchor system failure", *Geomech. Eng.*, **9**(6), 689-707
- Shen, B.T. (2014), "Coal mine roadway stability in soft rock: a case study", *Rock Mech. Rock Eng.*, **47**(6), 2225-2238.
- Tian, Z.C., Dong, L.H. and Liu, Y.J. (2013), *Numerical Simulation Analysis on Deformation Mechanism of Shallow-Buried Soft Rock Roadway*, in *Advanced Materials Research*, Trans Tech Publications, 773-776.
- Vlachopoulos, N. and Diederichs, M.S. (2014), "Appropriate uses and practical limitations of 2D numerical analysis of tunnels and tunnel support response", *Geotech. Geol. Eng.*, **32**(2), 469-488.
- Xia, C.C., Gui, Y., Wang, W. and Du, S.G. (2014), "Numerical method for estimating void spaces of rock joints and the evolution of void spaces under different contact states", *J. Geophys. Eng.*, **11**(6), 65004-65015.
- Xing, H.L., Makinouchi, A. and Zhao, C. (2008), "Three-dimensional finite element simulation of large-scale nonlinear contact friction problems in deformable rocks", *J. Geophys. Eng.*, **5**(1), 27-36.
- Yang, X.L. and Yan, R.M. (2015), "Collapse mechanism for deep tunnel subjected to seepage force in layered soils", *Geomech. Eng.*, **8**(5), 741-756
- Yu, W.J., Qu, Y.S. and Deng D.Q. (2013), *Supporting Numerical Simulation of Roadway Surrounding Rock in Deep High Stress*

Based on Broken-Expand Deformation, in *Applied Mechanics and Materials*, Trans Tech Publications, 1310-1314.

Zhang, B., Yu, X.L., Liu, N. and Zhu, F. (2013), *Numerical Simulation Research on Deep Soft Rock Roadway*, in *Applied Mechanics and Materials*, Trans Tech. Publications, 1439-1442.

Zhang, M.W., Shimada, H., Sasaoka, T., Matsui, K. and Dou, L.M. (2014), "Evolution and effect of the stress concentration and rock failure in the deep multi-seam coal mining", *Environ. Earth Sci.*, **72**(3), 629-643.

JS